

Hyperfine anomaly in the $z^6P_{7/2}$ level of the $4f^76s6p$ configuration of europium I

E. R. Eliel, K. A. H. van Leeuwen, and W. Hogervorst

Natuurkundig Laboratorium, Vrije Universiteit, 1081 HV Amsterdam, The Netherlands

(Received 25 February 1980)

The hyperfine interaction constants of the $z^6P_{7/2}$ and $z^8P_{7/2}$ levels of the configuration $4f^76s6p$ of the isotopes ^{151}Eu and ^{153}Eu have been remeasured with the laser-atomic-beam technique. The analysis yields values of $-6.80(26)\%$ and $-1.00(3)\%$, respectively, for the hyperfine anomalies. The anomaly in the $z^6P_{7/2}$ level is the largest so far observed and deviates considerably from the ground-state hyperfine anomaly. The experimental values of the hyperfine anomaly are compared with a calculation based on Nilsson-type nuclear wave functions. Possibly the electronic-state dependence of the hyperfine anomaly is due to core polarization.

INTRODUCTION

The study of hyperfine structure in an optical transition has long been an important tool for the determination of nuclear ground-state multipole moments. Precise measurements enable one to probe, for example, variations in the distribution of nuclear magnetization between various isotopes. The development of narrow-bandwidth light sources, i. e., tunable cw dye lasers, has considerably enlarged the possibility and accuracy of such hyperfine studies.

The hyperfine splittings in the levels of the even-parity configuration $(4f)^76s6p$ of neutral europium have been the subject of numerous investigations, the major part being limited to the isotope 151. Interferometric techniques have been used by Müller *et al.*,¹ Krüger and Lange,² and Kuhl;³ Lange⁴ and Champeau⁵ used the level-crossing technique. Recently a laser-atomic-beam high-resolution study has been performed by us⁶ yielding accurate hyperfine-interaction constants for 8 levels of this configuration for both ^{151}Eu and ^{153}Eu . For the $z^6P_{7/2}$ level we obtained hyperfine-interaction constants that differed significantly from the values obtained by Lange.⁴ This discrepancy together with a possibly large hyperfine anomaly stimulated a more accurate study of this level.

In this paper we report accurate measurements of the hyperfine-interaction constants in the excited states $z^6P_{7/2}$ and $z^8P_{7/2}$, using an atomic beam and a cw dye laser. The importance of correcting the experimental results for second-order hyperfine interactions is demonstrated. The hyperfine anomaly in these levels, as calculated from the corrected hyperfine-interaction constants, is compared with the result of a calculation based on Nilsson-type wave functions for the nucleus.

EXPERIMENTAL SETUP AND PROCEDURE

In the experimental setup the beam of a narrow-bandwidth laser orthogonally intersects a highly collimated atomic beam. The laser, a tunable cw dye ring laser, pumped by a cw Ar^+ laser (Spectra Physics 380A and 171, respectively) is, in order to reduce the effective laser-bandwidth, frequency locked on a wing of a transmission peak of a highly stable confocal Fabry-Perot interferometer (Burleigh CF 125). The frequency stabilization circuit consists of two feedback loops. The error signal—the difference between a signal proportional to the power output and a signal proportional to the power transmitted by the etalon—is, after amplification, applied directly to a piezoelectric crystal. This piezoelectric crystal serves as a mirror mount for one of the laser mirrors, which has been thinned down to increase the high-frequency response. In the second loop the error signal is integrated and fed back to the galvo of the ring laser, taking care of the large drift and low-frequency jitter. In this way we have been able to reduce the laser bandwidth to <2 MHz; the limiting factor is the frequency cutoff (50 kHz) of the high-voltage amplifier for the piezoceramic.

The atomic beam, produced by heating a tantalum oven using electron bombardment to a temperature of about 1000 K, is strongly collimated, resulting in a Doppler width of <1 MHz. The laser beam perpendicularly intersects the atomic beam and the fluorescent light is collected and focused on a photomultiplier (EMI 9789QA). Care has been taken to minimize stray light from the laser beam and from the oven. The laser frequency is adjusted to within 1 GHz at the atomic transition frequency with the help of a Michelson interferometer-type wavelength meter. A frequency scan (maximum 5 GHz) is made by varying the length of the locking etalon. To calibrate the

scan a set of frequency markers is recorded simultaneously with the atomic absorption spectrum. These markers are produced by recording the transmission of a highly stable confocal Fabry-Perot interferometer (Burleigh CF1500), which has a free spectral range of ~ 150 MHz. The photomultiplier signal is fed to a photon counter and is transferred, together with the calibration signal, to a minicomputer, enabling storage and further data handling.

We have studied the transitions at $\lambda = 576.520$ nm to the $z^6P_{7/2}$ level and at $\lambda = 626.696$ nm to the $z^8P_{7/2}$ level, the former level being of great interest for the study of the hyperfine anomaly. The $z^8P_{7/2}$ level has been included as a reference as it exhibits a less complicated hyperfine spectrum. In the 576.520-nm transition of Eu the spectra of the two isotopes are completely separated, each isotope spanning only 300 MHz approximately, while their separation is ~ 3.3 GHz. Spectra of the two isotopes (natural abundancies 47.8% and 52.2% for 151 and 153, respectively) consisting of 16 hyperfine components each are shown in Fig. 1. The necessity of a small instrumental linewidth

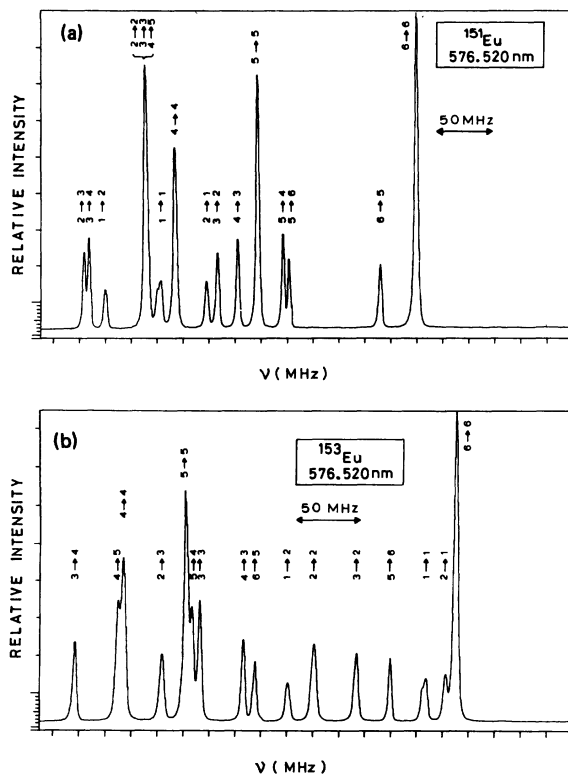


FIG. 1. The transition at 576.520 nm of Eu I. The hyperfine components are indicated by the values of the total angular momentum of ground and excited state. The upper number belongs to the excited state.

is obvious. The experimental linewidth of ~ 3 MHz, still larger than the natural linewidth (1.2 MHz FWHM),⁷ is, in addition to this natural width, composed of laser bandwidth, Zeeman broadening due to stray magnetic fields, and residual Doppler width. To minimize the latter, care has been taken that laser beam and atomic beam intersect perpendicularly by searching for the smallest experimental linewidth while changing the relative angle slightly. The Zeeman contribution, whose presence is clearly visible in the splitting of the $F=1 \rightarrow F'=1$ transitions in Fig. 1, has been reduced in later experiments with the help of three mutually orthogonal sets of Helmholtz coils.

The experimental data have been analyzed as follows. The spectrum was linearized by fitting a polynomial of order ≤ 4 to the calibration peak separations. A computer analysis of the linearized experimental spectrum allowed for the accurate determination of the frequency intervals between the various peaks and the separation of some badly resolved peaks. The line shape was assumed to be Gaussian. Sixteen different experimental spectra, recorded on three separate occasions, have been used in the analysis. The theoretical intensity distribution reproduces accurately the experimental intensities, corroborating the assignment of the peaks. From the positions of the peaks in each spectrum both the ground- and excited-state magnetic-dipole and electric-quadrupole hyperfine interaction constants A and B have been determined. The ground-state values are within experimental error in accordance with the results of atomic beam magnetic resonance (ABMR) measurements.⁸ A determination of the excited-state interaction constants, with the ground-state interaction constants fixed on the ABMR values, results in a fit between experimental and calculated hyperfine splittings of equal quality. This corroborates the calibration of the interferometer, which is based upon experiments on Na, Tm, and Dy.

The resulting excited-state interaction constants A and B (typical errors are 20 and 450 kHz, respectively) have been averaged and the final results are displayed in Table I. The errors correspond to three times the statistical error. No

TABLE I. The magnetic-dipole and electric-quadrupole interaction constants of the $4f^7 6s 6p z^6P_{7/2}$ level. The errors correspond to 3 times the statistical error.

Isotope	A (MHz)	B (MHz)
^{151}Eu	-6.196(8)	133.43(13)
^{153}Eu	-2.986(6)	322.00(28)

systematic differences have been found between the results of the three different runs although the laser linewidth and the Zeeman broadening differed slightly from run to run.

THEORY

The hyperfine splitting of atomic energy levels is caused by the interaction of the electrons with the nuclear magnetization and the nonspherical nuclear charge distribution. For all but the most accurate measurements the hyperfine interaction can be described very well by the magnetic-dipole and electric-quadrupole interaction, and the results expressed in terms of nuclear magnetic-dipole and electric-quadrupole moments. The finite electron probability density within the dimensions of the nucleus enables one to probe differences in the nuclear magnetization distribution

between two isotopes, the measurable effect whereof is, if the nuclear moments are known, commonly expressed by the hyperfine anomaly parameter.

Neglecting this small effect the Hamiltonian describing the hyperfine interaction can be written in the form⁹

$$H_{\text{hfs}} = \sum_k T_e^{(k)} \cdot T_n^{(k)}, \quad (1)$$

where $T_e^{(k)}, T_n^{(k)}$ are tensors of rank k acting on electronic and nuclear coordinates, respectively. The hyperfine interaction couples the electronic angular momentum \vec{J} with the nuclear spin \vec{I} to a total angular momentum \vec{F} . Using first-order perturbation theory the perturbation energy due to the hyperfine interaction equals

$$\begin{aligned} \langle \alpha I J F_M_F | H_{\text{hfs}} | \alpha I J F_M_F \rangle &= (-1)^{I+J+F} \sum_k \begin{Bmatrix} J & I & F \\ I & J & k \end{Bmatrix} \langle \gamma J || T_e^{(k)} || \gamma J \rangle \langle \beta I || T_n^{(k)} || \beta I \rangle \\ &= (-1)^{I+J+F} \sum_k A_k \frac{\begin{Bmatrix} J & I & F \\ I & J & k \end{Bmatrix}}{\begin{bmatrix} J & k & J \\ -J & 0 & J \end{bmatrix} \begin{bmatrix} I & k & I \\ -I & 0 & I \end{bmatrix}}, \end{aligned} \quad (2)$$

where the A_k factors are related to the well-known multipole-coupling constants¹⁰

$$\begin{aligned} A &= \frac{A_1}{IJ} = \frac{\mu_I}{I[J(J+1)(2J+1)]^{1/2}} \langle J || T_e^{(1)} || J \rangle, \\ B &= 4A_2 = 2eQ \left(\frac{J(2J-1)}{(2J+3)(2J+1)(J+1)} \right)^{1/2} \langle J || T_e^{(2)} || J \rangle, \\ C &= A_3, \\ D &= A_4, \end{aligned} \quad (3)$$

where μ_I and Q are the nuclear magnetic-dipole and electric-quadrupole moments, respectively.

An accurate description of the hyperfine interaction requires the use of relativistic electronic wave functions. Sandars and Beck¹¹ have shown that the use of an effective hyperfine Hamiltonian supersedes the necessity of relativistic wave functions and enables one to use LS -coupled nonrelativistic wave functions as basis functions. The effective Hamiltonian has the same form as Eq. (1). The electronic part of the magnetic-dipole and electric-quadrupole operators can be written in the form¹²

$$\begin{aligned} T_e^{(1)} &= \frac{2\mu_0\mu_B}{4\pi} \sum_{i=1}^N [s_i \langle r_i^{-3} \rangle_{10} - \sqrt{10} (s_i C_i^{(2)})^{(1)} \langle r_i^{-3} \rangle_{12} + l_i \langle r_i^{-3} \rangle_{01}], \\ T_e^{(2)} &= \frac{e}{4\pi\epsilon_0} \sum_{i=1}^N \{ -C_i^{(2)} \langle r_i^{-3} \rangle_{02} + [s_i (C_i^{(4)} l_i)^{(3)}]^{(2)} \langle r_i^{-3} \rangle_{13} + (s_i l_i)^{(2)} \langle r_i^{-3} \rangle_{11} \}, \end{aligned} \quad (4)$$

where the summation extends over all electrons outside the closed shells, μ_B is the Bohr magneton, and the quantities $\langle r_i^{-3} \rangle_{kl}$ are relativistic radial integrals. l_i , s_i , and $(s_i C_i^{(2)})^{(1)}$ are the one-electron orbital-, spin-, and spin-dipole operators,

respectively. In the nonrelativistic limit

$$\begin{aligned} \langle r_i^{-3} \rangle_{12} &= \langle r_i^{-3} \rangle_{01} = \langle r_i^{-3} \rangle_{02}, \\ \langle r_i^{-3} \rangle_{13} &= \langle r_i^{-3} \rangle_{11} = 0, \end{aligned}$$

$$\langle r_i^{-3} \rangle_{10} = 4\pi \langle \delta(r) \rangle,$$

where $\delta(r)$ is the Dirac delta function.

The evaluation of the radial integrals requires the knowledge of the radial part of the wave functions. Lindgren and Rosén¹³ have calculated these radial integrals for all the rare-earth atoms with various Hartree-Fock methods. A different approach is to consider the radial integrals as free parameters, to be determined from a fit to the experimental data. In that approach, in the case of europium, experimental values of at least 5 A factors and 2 B factors are required for the configuration $(4f)^7 6s6p$. A reduction of the number of unknown radial integrals is necessary if less data are available and is made by mutually relating some radial integrals using relativistic correction factors¹⁰ or the ratios of calculated radial integrals.¹³ The free-parameter approach implicitly incorporates such effects as configuration interaction and core polarization. For convenience one defines the so-called one-electron hyperfine parameters

$$\begin{aligned} a_{kl}(i) &= \frac{2\mu_0}{4\pi} \frac{\mu_I}{I} \mu_B \langle r_i^{-3} \rangle_{kl}, \quad kl = 01, 10, 12, \\ b_{kl}(i) &= \frac{e^2 Q}{4\pi \epsilon_0} \langle r_i^{-3} \rangle_{kl}, \quad kl = 02, 13, 11. \end{aligned} \quad (5)$$

The experimental hyperfine-interaction constants A and B can then be expressed as a linear combination of these one-electron hyperfine parameters, the coefficients in the expansion being the matrix elements of the tensor operators in Eq. (4) between the angular parts of the wave functions.

Equation (3) implies that the ratio of the hyperfine-interaction constants A for two isotopes equals the ratio of the nuclear gyromagnetic ratios $g_I = \mu_I/I$. This equality, however, is not exactly fulfilled since the finite extension of the nucleus and the distribution of nuclear magnetization have been neglected in this simple treatment. The deviation from the simple result is expressed in the hyperfine anomaly ${}^1\Delta^2$, where

$${}^1\Delta^2 = 1 - \frac{A(1)g_I(2)}{A(2)g_I(1)}. \quad (6)$$

Hyperfine anomalies are generally small, at most a few percent.¹⁴ To our knowledge no unambiguous quadrupole anomaly¹⁵ has been found.

Before calculating the hyperfine anomaly ${}^1\Delta^2$ from the experimental A values and gyromagnetic ratios it is necessary to correct the A values for second-order effects, i.e., to calculate the hyperfine energy up to second order in perturbation theory. The second-order hyperfine energy equals

$$\begin{aligned} E^{(2)} &= \sum_k (-1)^{I+J+F} \left\{ \begin{matrix} J & I & F \\ & J & k \end{matrix} \right\} \sum_{p,q,\alpha'J'+\alpha J} (-1)^{2I+2J+2k+p+q} (2k+1) \left\{ \begin{matrix} p & q & k \\ J & J & J' \end{matrix} \right\} \left\{ \begin{matrix} p & q & k \\ I & I & I \end{matrix} \right\} \frac{1}{E_{\alpha J} - E_{\alpha' J'}} \\ &\quad \times \langle \alpha J || T_{\sigma}^{(p)} || \alpha' J' \rangle \langle \alpha' J' || T_{\sigma}^{(q)} || \alpha J \rangle \langle I || T_n^{(p)} || I \rangle \langle I || T_n^{(q)} || I \rangle, \end{aligned} \quad (7)$$

where the summation extends over all electronic levels except αJ and we assume that the hyperfine interaction does not mix the nuclear levels. The $k=1$ and $k=2$ terms can be written in a form that shows directly the correction to the hyperfine-interaction constants A_k :

$$\begin{aligned} \delta A_k &= \sum_{p,q} \left[\begin{matrix} J & k & J \\ -J & k & J \end{matrix} \right] \left[\begin{matrix} I & k & I \\ -I & 0 & I \end{matrix} \right] \sum_{\alpha' J' + \alpha J} (-1)^{2I+2J+2k+p+q} \frac{(2k+1)}{E_{\alpha J} - E_{\alpha' J'}} \left\{ \begin{matrix} p & q & k \\ I & I & I \end{matrix} \right\} \left\{ \begin{matrix} p & q & k \\ J & J & J' \end{matrix} \right\} \\ &\quad \times \langle \alpha J || T_{\sigma}^{(p)} || \alpha' J' \rangle \langle \alpha' J' || T_{\sigma}^{(q)} || \alpha J \rangle \langle I || T_n^{(p)} || I \rangle \langle I || T_n^{(q)} || I \rangle. \end{aligned} \quad (8)$$

A calculation of these corrections requires the knowledge of the one-electron hyperfine parameters a_{kl} and b_{kl} .

The effects on the hyperfine interaction of an extended nucleus relative to a point nucleus are, as stated above, expressed by the hyperfine anomaly parameter. The finite extension of the nucleus, to which only penetrating electrons (s and $p_{1/2}$) are sensitive, results in a correction to the hyperfine-interaction parameters for a point nucleus. The relative effect of the distributed nuclear magnetization is known as the Bohr-Weisskopf anomaly ϵ_{BW} .^{16,17} An extended nuclear charge with a pointlike magnetization also introduces a correction to the hyperfine interaction parameters, known as the Breit-Rosenthal-Crawford-Schawlow correction ϵ_{BR} .^{18,19} The corrected result is

$$A = A_{\text{point}} (1 + \epsilon_{BW}) (1 + \epsilon_{BR}). \quad (9)$$

The extended-charge correction has been calculated for a diffuse (Hofstadter) nuclear charge distribution by Rosenberg and Stroke.¹⁹ The calculation of the Bohr-Weisskopf anomaly requires the knowledge of the nuclear wave function. Describing the nuclear ground state by a superposition of Nilsson wave functions^{20,21}

$$|\Psi\rangle = \sum_j C_j |Nlj\Omega\rangle, \quad (10)$$

one can write²² ($\Omega \neq \frac{1}{2}$)

$$\epsilon = -\frac{1}{\mu_I} \frac{I}{I+1} \left(\sum_{j'j} (-1)^{I-j} C_j C_{j'} \begin{bmatrix} j & 1 & j' \\ -I & 0 & I \end{bmatrix} \left\{ \sum_{t=1}^2 \left[g_L (b_L)_{2t} \langle j || L \left(\frac{r}{R_0} \right)^{2t} || j' \rangle + g_S (b_S)_{2t} \langle j || S \left(\frac{r}{R_0} \right)^{2t} || j' \rangle + g_D (b_D)_{2t} \langle j || \left(\frac{r}{R_0} \right)^{1/2} (S C^{(2)})^{(1)} \left(\frac{r}{R_0} \right)^{2t} || j' \rangle \right] \right\} + g_R \sum_{t=1}^2 (b_L)_{2t} \nu_t \right), \quad (11)$$

where μ_I is the nuclear magnetic moment expressed in nuclear magnetons, I is the nuclear spin, and g_L , g_S , and g_R are the orbital, spin, and rotational g factors, respectively. The atomic parameters $(b_L)_{2t}$, $(b_S)_{2t}$, and $(b_D)_{2t}$ are defined by Stroke *et al.*¹⁹ and can be extracted from their tables for s and $p_{1/2}$ electrons. The parameter ν_1 has been introduced by Reiner²³ to account for the influence of the collective nuclear rotation on the radial distribution of the nuclear current density. The equivalent parameter ν_2 is taken to be $0.8\nu_1$.²⁴ The reduced matrix elements in Eq. (11) can be written as

$$\langle Nlj || M_{\text{op}}(r/R_0)^{2t} || Nl'j' \rangle = \langle Nlj || M_{\text{op}} || Nl'j' \rangle (\sigma)^t \frac{\langle Nl | r^{2t} | Nl' \rangle}{\langle Nl | r^{2t} | Nl' \rangle}, \quad (12)$$

where $\sigma = (R_0)^{-2} \langle Nl | r^{2t} | Nl' \rangle$, and are calculated in a straightforward manner using harmonic oscillator wave functions and standard angular-momentum theory. The total hyperfine anomaly for a single electron can now be written as

$${}^1\Delta^2 \sim \epsilon_{\text{BW}}(1) - \epsilon_{\text{BW}}(2) + \epsilon_{\text{BR}}(1) - \epsilon_{\text{BR}}(2), \quad (13)$$

where, generally,¹⁹

$$\epsilon_{\text{BW}}(1) - \epsilon_{\text{BW}}(2) \gg \epsilon_{\text{BR}}(1) - \epsilon_{\text{BR}}(2).$$

DISCUSSION

The results for the $z^6P_{7/2}$ level, as shown in Table I, are a factor of 10 more accurate than previously published values.^{4,6} However, they markedly differ from the results obtained by Lange⁴ in a level-crossing experiment. We have calculated the line positions for the 576.520 nm transition with his values ${}^{151}A = -6.51(6)$ MHz, ${}^{151}B = 131.2(1.0)$ MHz, ${}^{153}A = -2.84(3)$ MHz, ${}^{153}B = 327.5(1.5)$ MHz, and the result is compared with our data in Fig. 2 using theoretical intensity ratios.¹⁰ The differences are most pronounced in the $F=5 \rightarrow F'=4$, $F=5 \rightarrow F'=6$ doublet and the $F=4 \rightarrow F'=5$, $F=3 \rightarrow F'=3$, $F=2 \rightarrow F'=2$ triplet. Lange's level crossing data for the isotope 151 are however reproduced better with ${}^{151}A = -6.3$ MHz, ${}^{151}B = 132$ MHz.⁶ The analysis of a level

crossing experiment requires the knowledge of the g_J factor of which no experimental value is known. Lange has used $g_J = 1.798$, calculated from the intermediate coupling functions of Bordarier *et al.*²⁵ The use of Smith's²⁶ wave functions results in $g_J = 1.775$. It might be suggested that the level-crossing data together with our new hyperfine-interaction constants can lead to an experimental value of g_J . However, the 2.65 Gauss level crossing $|4, 3\rangle \times |5, 5\rangle$ in ${}^{153}\text{Eu}^4$ cannot be reproduced by varying the g_J factor within reasonable limits.

For the calculation of the second-order corrections the one-electron hyperfine parameters a_{ki} and b_{ki} are required [Eq. (5)], which have been calculated as follows. With the intermediate-coupling electronic wave functions calculated by Smith²⁶ the matrix elements of the tensor operators in Eq. (4) have been evaluated. The Smith functions, which take into account configuration interaction, are mixtures of the configurations $(4f)^7 6s6p$, $(4f)^6 (6s)^2 5d$, and $(4f)^7 5d6p$, the $(4f)^7 6s6p$ contribution being dominant. We have restricted the analysis of the hyperfine interaction constants to those levels which have only a slight amount of

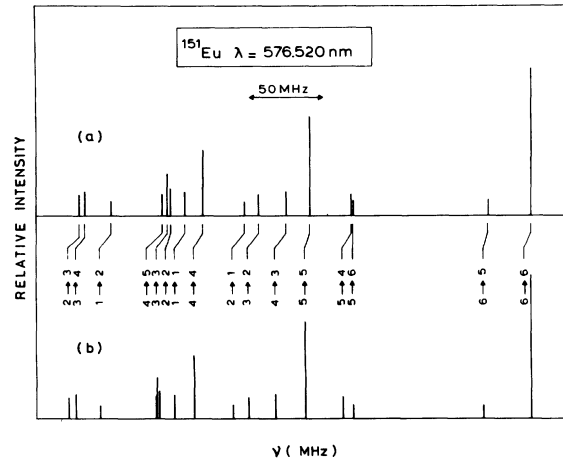


FIG. 2. The transition at 576.520 nm of ${}^{151}\text{Eu}$. Peak positions calculated with Lange's (Ref. 9) results (upper picture) and with present results (lower picture). Peak identification as in Fig. 1.

configuration interaction and are almost purely $(4f)^7 6s6p$. In the appropriate coupling scheme²⁷ the 7 f electrons are coupled to an 8S core, the s and p electrons to 3P or 1P resulting in 6P , 8P , and ^{10}P multiplets. In this coupling scheme the f electrons exhibit only a contactlike magnetic-dipole interaction and do not contribute to the electric-quadrupole interaction at all. This greatly simplifies the analysis.

The magnetic-dipole hyperfine interaction in configurations with an unpaired s electron is commonly dominated by the contact interaction of the s electron. This is also the case for europium. The small value for $A(z^6P_{7/2})$ is caused by the very small value of the "angular" coefficient of the $a_{10}(6s)$ parameter, a result of accidental cancellation of diagonal and off-diagonal matrix elements in the intermediate coupling calculation. This cancellation reduces the pure LS coupling value by a factor of 200.

The a_{k1} one-electron hyperfine parameters have been extracted from the expression²⁸

$$A_{\text{exp}} = \alpha a_{10}(4f) + \beta a_{10}(6s) + \gamma a_{10}(6p) + \delta a_{01}(6p) + \epsilon a_{12}(6p). \quad (14)$$

For the isotope 151 the a_{k1} parameters have been determined from a least-squares fit to the experimental A factors of seven levels which are almost purely $(4f)^7 6s6p$ (see Table II). The parameter $a_{10}(6p)$ has been discarded by relating its value to the value of $a_{01}(6p)$ using Kopfermann's relativistic correction factor $-0.095 (Z_{\text{eff}} = Z - 4)$.¹⁰ For the other isotope two alternative procedures are possible. The same procedure as for the 151 isotope can be followed. In this case only 5 experimental A factors are available to evaluate 4 parameters. Alternatively, neglecting the hyperfine anomaly the one-electron hyperfine parameters $^{153}a_{k1}$ and $^{151}a_{k1}$ can be related using the ratio of the gyromagnetic ratios $^{153}a_{k1}/^{151}a_{k1} = ^{153}g_I/^{151}g_I$. Both approaches have been followed, resulting in only slightly different one-electron hyperfine parameters for the isotope 153. In Table II the results are given for the first procedure.

The b_{k1} parameters have been extracted from the expression

$$B_{\text{exp}} = \mu b_{11}(6p) + \nu b_{02}(6p); \quad (15)$$

7 and 5 experimental values are available for the isotopes 151 and 153, respectively. The direct

TABLE II. Analysis of the hyperfine-interaction constants. The table gives experimental hyperfine-interaction constants, second-order corrections, corrected hyperfine-interaction constants, and the results of the effective-operator formalism calculation (all in MHz). The errors in the experimental values correspond to the statistical error. Experimental data for the $z^8P_{5/2}$, $z^8P_{7/2}$, and $z^6P_{5/2}$ are from Ref. 6; for the $z^{10}P$ levels from Ref. 1.

Level	¹⁵¹ Eu							
	¹⁵¹ A _{expt}	¹⁵¹ δA	¹⁵¹ A _{corr}	¹⁵¹ A _{calc}	¹⁵¹ B _{expt}	¹⁵¹ δB	¹⁵¹ B _{corr}	¹⁵¹ B _{calc}
$z^8P_{5/2}$	-606.8(4)	0.0104(1)	-606.8(4)	-600.3	65(4)	-1.48(2)	66.5(4.0)	66.9
$z^8P_{7/2}$	-236.12(1)	0.0175(2)	-236.14(1)	-236.3	-202.1(2)	-4.28(4)	-197.8(2)	-192.7
$z^8P_{9/2}$	664.9(5)	0.0924(9)	664.9(5)	675.1	296(7)	5.47(6)	291(7)	289.4
$z^6P_{5/2}$	-590.7(5)	0.3226(32)	-591.0(5)	-602.7	-354(4)	-4.09(4)	-350(4)	-372.4
$z^6P_{7/2}$	-6.096(2)	0.3329(33)	-6.429(4)	-7.0	133.43(6)	7.84(8)	125.59(7)	138.3
$z^{10}P_{7/2}$	968.6(6)	0.0548(5)	968.6(6)	962.6	157.3(6.0)	2.51(2)	154.8(6.0)	160.2
$z^{10}P_{9/2}$	1023.1(3)	0.0613(6)	1023.0(3)	1023.6	-503.2(3.0)	2.91(3)	-506.2(3.0)	-493.2
		$a_{10}(4f) =$	-78.3(3.3) MHz		$b_{11}(6p) =$	-70(16) MHz		
		$a_{10}(6s) =$	10 065(48) MHz		$b_{02}(6p) =$	1071(20) MHz		
		$a_{01}(6p) =$	442(22) MHz					
		$a_{12}(6p) =$	862(31) MHz					
Level	¹⁵³ Eu							
	¹⁵³ A _{expt}	¹⁵³ δA	¹⁵³ A _{corr}	¹⁵³ A _{calc}	¹⁵³ B _{expt}	¹⁵³ δB	-corr	¹⁵³ B _{calc}
$z^8P_{5/2}$	-268.6(3)	0.0109(3)	-268.6(3)	-268.4	166(3)	-0.17(1)	166(3)	167.6
$z^8P_{7/2}$	-105.30(1)	0.0036(6)	-105.31(1)	-106.2	-505.2(2)	-0.78(1)	-504.4(2)	-480.4
$z^8P_{9/2}$	294.9(2)	0.0115(1)	294.9(2)	294.2	725(3)	1.20(1)	724(3)	714.1
$z^6P_{5/2}$	-263.3(3)	0.0855(2)	-263.2(3)	-264.4	-919(3)	-0.63(1)	-920(3)	-932.1
$z^6P_{7/2}$	-2.986(2)	0.0587(2)	-3.045(2)	-2.49	322.0(1)	1.83(2)	320.2(1)	327.1
		$a_{10}(4f) =$	-38.0(8) MHz		$b_{11}(6p) =$	-147(26) MHz		
		$a_{10}(6s) =$	4375(21) MHz		$b_{02}(6p) =$	2653(41) MHz		
		$a_{01}(6p) =$	208.3(4.1) MHz					
		$a_{12}(6p) =$	361.8(6.2) MHz					

analysis for both isotopes yields one-electron hyperfine parameters $b_{11}(6p)$ and $b_{02}(6p)$ whose isotopic ratios are, within the limits of error, in accordance with the ratio of the $^8S_{7/2}$ ground-state electric-quadrupole hyperfine-interaction constants.⁸

Once the one-electron hyperfine parameters are known the second-order corrections can be evaluated, again using Smith's wave functions. In the calculation, made with the computer program ZWORD, only the nearby levels of the $(4f)^76s6p$ configuration, i. e., the z^6P , z^8P , $z^{10}P$, and y^8P multiplets, have been taken into account. Only the dipole-dipole, dipole-quadrupole, and quadrupole-quadrupole contributions to δA_k are of importance and have been evaluated. Due to the large value of $a_{10}(6s)$ the dipole-dipole contribution is by far the most important. The corrections, shown in Table II, have been evaluated only for the $(4f)^76s6p$ part of the wave function. This is a good approximation since all the z^P terms are at least 98.2% pure $(4f)^76s6p$, and the contribution of the remaining two configurations is, in the absence of an unpaired s electron, expected to be small, even in levels with a relatively large amount of configuration interaction. As the second-order corrections are of the order of a MHz and most pronounced in the $z^6P_{7/2}$ level, the extraction of the one-electron hyperfine parameters has been repeated, now from the corrected hyperfine-interaction constants. This second set of hyperfine parameters has been used to recalculate the second-order corrections. The difference between the first and second set of corrections is of the order of 1 kHz only. Inclusion of higher multipole moments does not modify the final values of the A and B factors.

In Table II we list the experimental A and B factors, the second-order corrections (second set), the corrected A and B factors, and the values calculated from the resultant one-electron hyperfine parameters. The experimental results for the $z^8P_{5/2}$, $z^8P_{9/2}$, and $z^6P_{5/2}$ levels are from Ref. 6. The results for the $z^{10}P_{7/2}$ and $z^{10}P_{9/2}$ levels of

^{151}Eu have been taken from Ref. 1, whereas the $z^6P_{7/2}$ and $z^8P_{7/2}$ levels have been remeasured in the present experiment. The agreement between the calculated and corrected experimental ^{151}A factors (rms deviation = 17 MHz) has improved compared to Lange's analysis⁴ (rms deviation = 25 MHz). An equal improvement is observed in the analysis of the ^{151}B factors compared to the analysis of Champeau *et al.*⁵ (rms deviations 29 MHz and 37 MHz, respectively). This improvement can be traced back to the exclusion of the y^8P levels, with a considerable contribution of the $(4f)^75d6p$ configuration, from the present analysis. The values of the a_{ki} and b_{ki} parameters, however, do not differ appreciably from Lange's and Champeau's values. The errors in the values of $^{151}\delta A$ and $^{151}\delta B$ reflect directly the 0.5% error in the value of $a_{10}(6s)$. The errors in the values of $^{153}\delta A$ and $^{153}\delta B$ are a measure of the difference between the results of the two approaches mentioned before. The values themselves are equal to the arithmetic mean of the two results.

Table III lists the ratios of the corrected A and B factors of ^{151}Eu and ^{153}Eu together with the ratios of nuclear magnetic-dipole moments and ground-state electric-quadrupole interaction constants and the derived hyperfine anomalies (HFA) for the $z^6P_{7/2}$ and $z^8P_{7/2}$ levels. The ratio of the corrected B factors agrees very well with the ground-state ratio and no quadrupole anomaly is observed. The magnetic-dipole hyperfine anomaly in the $z^6P_{7/2}$ level belongs to the largest so far observed and deviates considerably from the ground-state hyperfine anomaly (~ 0).²⁹

The calculation of the hyperfine anomaly proceeds as follows. The Breit-Rosenthal-Crawford-Schawlow correction ϵ_{BR} for a Hofstadter-type nuclear charge distribution has been extracted from the table of Rosenberg and Stroke,¹⁹ $\epsilon_{\text{BR}}(151) - \epsilon_{\text{BR}}(153) = +0.012\%$. The Bohr-Weisskopf anomaly has been calculated with the help of Eq. (11). For ^{151}Eu ($I = \frac{5}{2}$) we used the Nilsson wave function for the $\frac{5}{2}^+[402]$ orbital^{21,30} with a deformation parameter $\beta = 0.14$ ³¹ and the known value of

TABLE III. The ratios of the corrected magnetic-dipole and electric-quadrupole hyperfine-interaction constants for the $z^6P_{7/2}$ and $z^8P_{7/2}$ level, together with the ratio of the magnetic moments (Ref. 29) and ground-state electric-quadrupole hyperfine-interaction constants (Ref. 8). The last column gives the differential hyperfine anomaly. Errors are calculated using three times statistical errors in the experimental data.

Level	$^{151}\text{A}/^{153}\text{A}_{\text{corr}}$	$^{151}\mu/^{153}\mu$	$^{151}\text{B}/^{153}\text{B}_{\text{corr}}$	$^{151}\text{B}/^{153}\text{B}_{\text{grs}}$	$^{151}\Delta^{153}$
$z^6P_{7/2}$	2.111(6)	2.265 05(42)	0.3922(34)	0.3928(20)	-6.80(26)%
$z^8P_{7/2}$	2.242(7)		0.3918(13)		-1.00(3)%

the nuclear magnetic dipole moment $\mu_I = 3.463\,60(6)\mu_N$.²⁹ For $^{153}\text{Eu}(I=\frac{5}{2})$ the $\frac{5}{2}^+[413]^{30}$ orbital, with $\beta=0.21$ ³⁰ and $\mu_I=1.5292(8)\mu_N$, has been used. We took $g_L=1$, $g_s=0.6g_s^{\text{free}}=3.35$, $g_R=0.4$,³⁰ $\nu_1=0.7$,²³ and $\nu_2=0.56$.²⁴ With these wave functions and gyromagnetic ratios the nuclear magnetic moments are reproduced satisfactorily. The electronic parameters b_L , b_s , and b_D have been obtained by interpolation between the $Z=60$ and $Z=65$ values in the table of Stroke *et al.* assuming mass independence for $\Delta A=2$. This calculation yields

$$\begin{aligned}\epsilon_{\text{BW}}(151)_s &= 0.79\%, \\ \epsilon_{\text{BW}}(153)_s &= 0.73\%, \\ \epsilon_{\text{BW}}(151)_{p_{1/2}} &= 0.12\%, \\ \epsilon_{\text{BW}}(153)_{p_{1/2}} &= 0.11\%.\end{aligned}$$

Reiner²³ gives $\epsilon_{\text{BW}}(153)_s=0.6\%$ using the shell-

$$A(^6P_{7/2}) = 0.824\,54a_{10}(4f) - 0.000\,49a_{10}(6s) - 0.039\,99a_{10}(6p) + 0.203\,83a_{01}(6p) - 0.033\,89a_{12}(6p),$$

$$A(^6P_{7/2}) = 0.926\,54a_{10}(4f) - 0.033\,13a_{10}(6s) - 0.024\,56a_{10}(6p) + 0.119\,06a_{01}(6p) + 0.134\,56a_{12}(6p),$$

resulting in $^1\Delta^2(^6P_{7/2})=0.76\Delta\epsilon_{\text{BW}}^s$ and $^1\Delta^2(^6P_{7/2})=1.41\Delta\epsilon_{\text{BW}}^s$ where the small $p_{1/2}$ contribution to the HFA has been neglected and $\Delta\epsilon_{\text{BW}}^s = \epsilon_{\text{BW}}^s(151) - \epsilon_{\text{BW}}^s(153)$. The aforementioned ϵ_{BW}^s values yield values for $^{151}\Delta^{153}(^6P_{7/2})$ between 0.05% and 0.84% and $^{151}\Delta^{153}(^6P_{7/2})$ between 0.08% and 1.6%. It is seen that the result of the calculation of the Bohr-Weisskopf anomaly does not reproduce the experimental results for the $z\ ^6P_{7/2}$ level, i. e., the nuclear wave functions and parameters are unable to explain the experimental HFA.

The hyperfine anomaly of a pure 6s electron $^{151}\Delta_s^{153}$ can be extracted from the experimental anomaly, using^{11,25,34,35}

$$^{151}\Delta_s^{153} = (A_{\text{corr}}/A_s)^{151}\Delta_s^{153}. \quad (16)$$

A_s is the contribution to the A factor arising from the contact interaction of the unpaired 6s electron. Neglecting core polarization A_s is given by the product of $a_{10}(6s)$ with the angular coefficient β [Eq. (14)]. Substituting the values of $^{151}\Delta_s^{153}$ and A_{corr} from Tables II and III as well as the value of $A_s[-0.033\,13a_{10}(6s)]$ for the level $z\ ^6P_{7/2}$ results in $^{151}\Delta_s^{153}=-0.71(4)\%$. This value agrees within experimental error with the average over the three levels $z\ ^8P_{5/2}$, $z\ ^8P_{9/2}$, and $z\ ^6P_{5/2}$ [$-0.7(1)\%$], with the values for the $z\ ^{10}P_{9/2}$ [$-0.64(14)\%$] and the $z\ ^{10}P_{7/2}$ [$-0.64(10)\%$] levels²⁵ and Baker and William's value for the $^8S_{7/2}$ ground state of Eu^{++} [$-0.65(11)\%$].³⁵ However, for the level $z\ ^6P_{7/2}$ a value $^{151}\Delta_s^{153}=-8.8(4)\%$ is obtained [with $A_s=-0.000\,49a_{10}(6s)$], which does not add to

model state $g_{7/2}$; Crecelius³² calculates $\epsilon_{\text{BW}}(151)_s=1.3\%$ for the Nilsson state $\frac{5}{2}^+[402]$. A calculation based on the shell-model state $d_{5/2}$ yields $\epsilon_{\text{BW}}(151)_s=1.7\%$ using $g_s=g_s^{\text{free}}$, and $\epsilon_{\text{BW}}(151)_s=1.3\%$ using $g_s=0.6g_s^{\text{free}}$. The simple empirical formula of Moskowitz and Lombardi³³ $\epsilon = \alpha/\mu$ ($I=l\pm\frac{1}{2}$, l is the odd-particle orbital angular momentum), which has proved to be in good agreement with experimental results on Hg, Au, and Ir,³⁴ is not applicable to the case of europium. The Breit-Rosenthal correction is seen to be a factor 5 smaller than the calculated differential Bohr-Weisskopf anomaly of the s electron and will be omitted in the remaining discussion. The contribution of the s and $p_{1/2}$ differential anomalies to the total HFA is proportional to the respective contactlike contributions to the hyperfine-interaction constant A , which can be extracted from the parametric expressions

this consistent picture. This level is characterized by a very small contact hyperfine interaction due to canceling diagonal and off-diagonal matrix elements ($\beta=-0.000\,49$) which, however, accounts almost completely for A_{exp} indicating that the contributions of the p and f electrons cancel almost exactly. Alternatively, the anomalies can be made consistent with a value of $\beta=-0.0062$ for the $z\ ^6P_{7/2}$ level. A very slight change in the wave function can easily account for this change in β . However, to retain the satisfying correspondence between calculated and experimental hyperfine-interaction constants (see Table II) one has to modify the values of the remaining angular constants much more drastically. Thus in order to improve the consistency of $^{151}\Delta_s^{153}$ one has either to give up the consistency of the calculated and experimental A factor or one has to assume that the electronic wave function for this level is seriously in error. There is, however, no further indication that this wave function, as calculated by Smith, is less reliable than the others. The absence of a quadrupole anomaly after addition of the second-order corrections gives considerable support to this statement. The anomalous value of $^{151}\Delta_s^{153}(z\ ^6P_{7/2})$, which clearly is not of nuclear origin, is conjectured to be at least partially due to core polarization, but remains unexplained.

ACKNOWLEDGMENTS

We are indebted to B. Post and J. Bouma for their assistance during the measurements, Dr. G.

Smith for sending us details of his wave functions, and Dr. K. D. Böklen for his assistance in the calculation of the second-order corrections. We

gratefully acknowledge the Stichting voor Fundamenteel Onderzoek der Materie for partial financial support.

-
- ¹W. Müller, A. Steudel, and H. Walther, *Z. Phys.* **183**, 303 (1965).
²H. D. Krüger and W. Lange, *Phys. Lett.* **42A**, 293 (1972).
³J. Kuhl, *Z. Phys.* **242**, 66 (1971).
⁴W. Lange, *Z. Phys.* **A272**, 223 (1975); and thesis, Hannover, 1970 (unpublished).
⁵R. J. Champeau, E. Handrick, and H. Walther, *Z. Phys.* **260**, 361 (1973).
⁶G. J. Zaal, W. Hogervorst, E. R. Eliel, K. A. H. van Leeuwen, and J. Blok, *Z. Phys.* **A290**, 339 (1979).
⁷M. Gustavsson, H. Lundberg, L. Nilsson, and S. Svanberg, *J. Opt. Soc. Am.* **69**, 984 (1979).
⁸P. G. H. Sandars and G. K. Woodgate, *Proc. R. Soc. London, Ser. A* **257**, 269 (1960).
⁹C. Schwartz, *Phys. Rev.* **97**, 380 (1955).
¹⁰H. Kopfermann, *Nuclear Moments* (Academic, New York, 1958).
¹¹P. G. H. Sandars and J. Beck, *Proc. R. Soc. London, Ser. A* **289**, 97 (1965).
¹²L. Armstrong, Jr., *Theory of Hyperfine Structure of Free Atoms* (Wiley-Interscience, New York, 1971).
¹³I. Lindgren and A. Rosén, *Case Stud. At. Phys.* **4**, 197 (1974).
¹⁴H. H. Stroke, in *Atomic Physics I*, edited by B. Bederson, V. Y. Cohen, and F. M. Pichanick (Plenum, New York, 1969), p. 523; H. M. Foley, *ibid.*, p. 509.
¹⁵M. B. White, S. S. Alpert, S. Penselin, T. I. Moran, V. W. Cohen, and E. Lipworth, *Phys. Rev.* **137**, B477 (1965).
¹⁶A. Bohr and V. F. Weisskopf, *Phys. Rev.* **77**, 94 (1950).
¹⁷H. H. Stroke, R. J. Blin-Stoyle, and V. Jaccarino, *Phys. Rev.* **123**, 1326 (1961).
¹⁸J. E. Rosenthal and G. Breit, *Phys. Rev.* **41**, 459 (1932); M. F. Crawford and A. L. Schawlow, *ibid.* **76**, 1310 (1949).
¹⁹H. J. Rosenberg and H. H. Stroke, *Phys. Rev. A* **5**, 1992 (1972).
²⁰S. G. Nilsson, *K. Dan. Vidensk. Selsk. Mat. Fys. Medd.* **29**, 1 (1955).
²¹J. P. Davidson, *Collective Models of the Nucleus* (Academic, New York, 1968).
²²D. L. Clark, M. E. Cage, D. A. Lewis, and G. W. Greenlees, *Phys. Rev. A* **20**, 239 (1979).
²³A. S. Reiner, *Nucl. Phys.* **5**, 544 (1958).
²⁴I. Unna, *Phys. Lett.* **24B**, 499 (1967).
²⁵Y. Bordarier, B. R. Judd, and M. Klapisch, *Proc. R. Soc. London, Ser. A* **289**, 81 (1965).
²⁶G. Smith (private communication).
²⁷G. Smith and B. G. Wybourne, *J. Opt. Soc. Am.* **55**, 121 (1965).
²⁸Calculated with the computer program AUFSPA. Kindly supplied by Dr. H. Brand (Hanover). A missing statement has been added to the program.
²⁹L. Evans, P. G. H. Sandars, and G. K. Woodgate, *Proc. R. Soc. London, Ser. A* **289**, 114 (1965).
³⁰C. Ekström and I.-L. Lamm, *Phys. Scr.* **7**, 31 (1973).
³¹C. Ekström, S. Ingelmann, M. Olsmats, and B. Wannberg, *Phys. Scr.* **6**, 181 (1972).
³²G. Crecelius, *Z. Phys.* **256**, 155 (1972).
³³P. A. Moskowitz and M. Lombardi, *Phys. Lett.* **46B**, 334 (1973); T. Fujita and A. Arima, *Nucl. Phys. A* **254**, 513 (1975).
³⁴S. Büttgenbach, R. Dicke, and F. Träber, *Phys. Rev. A* **19**, 1383 (1979).
³⁵J. M. Baker and F. I. B. Williams, *Proc. R. Soc. London, Ser. A* **267**, 283 (1962).